Power Control in Cognitive Radio Networks: How to Cross a Multi-Lane Highway

Wei Ren, Qing Zhao, and Ananthram Swami

***Abstract*—We consider power control in cognitive radio networks where secondary users identify and exploit instantaneous and local spectrum opportunities without causing unacceptable interference to primary users. We qualitatively characterize the impacts of the transmission power of secondary users on the occurrence of spectrum opportunities and the reliability of opportunity detection. Based on a Poisson model of the primary network, we quantify these impacts by showing that (i) the probability of spectrum opportunity decreases exponentially with the transmission power of secondary users, where the exponential decay constant is given by the traffic load of primary users; (ii) reliable opportunity detection is achieved in the two extreme regimes in terms of the ratio between the transmission power of secondary users and that of primary users. Such analytical characterizations allow us to study power control for optimal transport throughput under constraints on the interference to primary users. Furthermore, we reveal the difference between detecting primary signals and detecting spectrum opportunities, and demonstrate the complex relationship between physical layer spectrum sensing and MAC layer throughput. The dependency of this PHY-MAC interaction on the application type and the use of handshake signaling such as RTS/CTS is also illustrated.**

***Index Terms*—Power Control, Cognitive Radio, Opportunistic Spectrum Access, Transport Throughput, Poisson Random Network.**

I. Introduction

THE BASIC idea of opportunistic spectrum access (OSA) is that spectrum efficiency and interoperability can be achieved through a hierarchical access structure with primary and secondary users. Secondary users, equipped with cognitive radios (CR) capable of sensing and learning the communication environment, can identify and exploit instantaneous and local spectrum opportunities without causing unacceptable interference to primary users [1]. Cognitive radios for OSA can address critical challenges in spectrum efficiency, interference management, and coexistence of heterogeneous networks in future generations of wireless systems [2].

While conceptually simple, CR for OSA presents new challenges in every aspect of the system design. In this paper, we focus on transmission power control. We show that unique features of CR systems give a fresh twist to this classic problem and call for a new set of fundamental theories and practical insights for the optimal design.

A. Power Control in Cognitive Radio Networks

In wireless networks, transmission power defines network topology and determines network capacity. The tradeoff between long-distance direct transmission and multi-hop relaying, both in terms of energy efficiency and network capacity, is now well understood in conventional wireless networks [3, 4].

This tradeoff in CR systems is, however, much more complex. The intricacies of power control in CR systems may be illustrated with an analogy of crossing a multi-lane highway, each lane having different traffic load. The objective is to cross the highway as fast as possible subject to a risk constraint. Should we wait until all lanes are clear and dash through, or cross one lane at a time whenever an opportunity arises? What if our ability to detect traffic in multiple lanes varies with the number of lanes in question?

We show in this paper that similar questions arise in power control for secondary users. The transmission power of a secondary user not only determines its communication range but also affects how often it sees spectrum opportunities. If a secondary user is to use a high power to reach its intended receiver directly, it must wait for the opportunity that no primary receiver is active within its relatively large interference region, which happens less often. If, on the other hand, it uses low power, it must rely on multi-hop relaying, and each hop must wait for its own opportunities to emerge.

A less obvious implication of the transmission power in CR networks is its impact on the reliability of opportunity detection. As shown in this paper, the transmission power of a secondary user affects the performance of its opportunity detector in terms of missed spectrum opportunities and collisions with primary users. Optimal power control in CR systems thus requires a careful analysis of the impacts of the transmission power on both the occurrence of opportunities and the reliability of opportunity detection.

B. Contributions

The key contribution of this paper lies in the characterization of the impacts of secondary users' transmission power on the occurrence of spectrum opportunities and the reliability of opportunity detection. These impacts of secondary users' transmission power lead to unique design tradeoffs in CR systems that are nonexistent in conventional wireless networks and have not been recognized in the literature on cognitive radio. The recognition and characterization of these tradeoffs

Manuscript received 30 August 2008; revised 31 January 2009. This work was supported in part by the Army Research Laboratory CTA on Communication and Networks under Grant DAAD19-01-2-0011, by the Army Research Office under Grant W911NF-08-1-0467, and by the National Science Foundation under Grants ECS-0622200 and CCF-0830685. Part of this work was presented at *ITA*, January 2008, and *ICASSP*, April 2008.

W. Ren and Q. Zhao are with the Department of Electrical and Computer Engineering, University of California, Davis, CA 95616 (e-mail: qzhao@ece.ucdavis.edu).

A. Swami is with the Army Research Laboratory, Adelphi, MD 20783.

Digital Object Identifier 10.1109/JSAC.2009.090923.

contribute to the fundamental understanding of CR systems and clarify two major misconceptions in the CR literature, namely, that the presence/absence of spectrum opportunities is solely determined by primary *transmitters* and that detecting primary signals is equivalent to detecting spectrum opportunities. We show in this paper the crucial role of primary receivers in the definition of spectrum opportunity, which results in the dependency of the occurrence of spectrum opportunities on the transmission power of *secondary users*, in addition to the well understood dependency on the transmission power of primary users. Furthermore, we show that spectrum opportunity detection is subject to error even when primary signals can be perfectly detected. This non-equivalence between detecting primary signals and detecting spectrum opportunities is the root for the connection between the reliability of opportunity detection and the transmission power of secondary users, a connection that has eluded the CR research community thus far.

The above qualitative and conceptual findings are general and applicable to various network and interference models. To quantify the impacts of secondary users' transmission power, we adopt a Poisson model of the primary network and a disk model for signal propagation and interference. Closed-form expressions for the probability of opportunity and the performance of opportunity detection (measured by the probabilities of false alarm and miss detection) are obtained. These closed-form expressions allow us to establish the exponential decay of the probability of opportunity with respect to the transmission power and the asymptotic behavior of the performance of opportunity detection. Specifically, we show that the probability of opportunity decreases exponentially with $p_{tx}^{2/\alpha}$, where p_{tx} is the transmission power of secondary users and α is the path-loss exponent. In terms of the impact of p_{tx} on spectrum sensing, we show that reliable opportunity detection is achieved in the *two extreme regimes of the ratio between the transmission power p_{tx} of secondary users and the transmission power P_{tx} of primary users: $\frac{p_{tx}}{P_{tx}} \to 0$ and $\frac{p_{tx}}{P_{tx}} \to \infty$.* These quantitative characterizations lead to a systematic study of optimal power control in CR systems. Adopting the performance measure of transport throughput, we examine how a secondary user should choose its transmission power according to the interference constraint, the traffic load and transmission power of primary users, and its own application type (e.g., guaranteed delivery vs. best-effort delivery).

While the disk propagation and interference model is simplistic, it leads to clean tractable solutions that highlight the main message regarding the dependencies of the definition, the occurrence, and the detection of spectrum opportunities on the transmission power of secondary users. It is our hope that this paper provides insights and initial results for characterizing such dependencies under more complex and more realistic network and interference models.

Other interesting findings include the difference between detecting primary signals and detecting spectrum opportunities and how it affects the performance of spectrum sensing. Furthermore, we demonstrate the complex relationship between physical layer spectrum sensing and MAC layer throughput. The dependency of this PHY-MAC interaction on the application type and the use of handshake signaling such as RTS/CTS is illustrated.

C. Related Work

Power control in conventional wireless networks has been well studied in the literature (see [3–6] and references therein). The impact of transmission power on network performance, such as delay, connectivity, network throughput, is summarized in [5, 7].

While there is a growing body of literature on power control in CR systems, the unique design tradeoffs in power control in CR systems, namely, the impacts of transmission power on the occurrence of opportunities and the reliability of opportunity detection, have not been recognized or analytically characterized in the literature.

In [8, 9], power control for one pair of secondary users coexisting with one pair of primary users is considered. The use of soft sensing information for optimal power control is explored in [8] to maximize the capacity/SNR of the secondary user under a peak power constraint at the secondary transmitter and an average interference constraint at the primary receiver. In [9], the secondary transmitter adjusts its transmission power to maximize its data rate without increasing the outage probability at the primary receiver. It is assumed in [9] that the channel gain between the primary transmitter and its receiver is known to the secondary user. In [10], a power control strategy based on dynamic programming is developed for one pair of secondary users under a Markov model of primary users' spectrum usage. Power control for OSA in TV bands is investigated in [11, 12], where the primary users (TV broadcast) transmit all the time and spatial (rather than temporal) spectrum opportunities are exploited by secondary users.

D. Organization and Notation

The rest of this paper is organized as follows. Sec. II provides a qualitative characterization of the impacts of transmission power in CR systems, and lays out the conceptual foundation for subsequent sections. In Sec. III, closed-form expressions and properties of the probability of spectrum opportunity and the performance of opportunity detection are obtained as functions of the transmission power p_{tx} based on a Poisson primary network model. Based on these analytical results, we study power control for optimal transport throughput in Sec. IV. The impacts of RTS/CTS handshake signaling on the performance of opportunity detection and the optimal transmission power are examined in Sec. V. Conclusions and further discussions are given in Sec. VI.

Throughout the paper, we use capital letters for parameters of primary users and lowercase letters for secondary users.

II. Impact of Transmission Power: Qualitative Characterization

This section lays out the conceptual foundation for subsequent sections. The impact of transmission power on the occurrence of opportunities is revealed through a careful examination of the definitions of spectrum opportunity and interference constraint. The impact of transmission power on the reliability of opportunity detection is demonstrated by illuminating the difference between detecting primary signals and detecting spectrum opportunities.

A. Impact on the Occurrence of Spectrum Opportunity

A formal investigation of CR systems must start from a clear definition of spectrum opportunity and interference constraint. To protect primary users, an interference constraint should specify at least two parameters $\{\eta,\ \zeta\}$. The first parameter η is the maximum allowable interference power perceived by an active primary receiver; it specifies the noise floor and is inherent to the definition of spectrum opportunity as shown below. The second parameter ζ is the maximum outage probability that the interference at an active primary receiver exceeds the noise floor η. Allowing a positive outage probability ζ is necessary due to opportunity detection errors. This parameter is crucial to secondary users in making transmission decisions based on imperfect spectrum sensing as shown in [13].

Spectrum opportunity is a local concept defined with respect to a particular secondary transmitter and its receiver for unicast. Intuitively, *a channel is an opportunity to a pair of secondary users if they can communicate successfully without violating the interference constraint*[1]. In other words, the existence of a spectrum opportunity is determined by *two logic conditions*: the reception at the secondary receiver being successful and the transmission from the secondary transmitter being "harmless". Deceptively simple, this definition has significant implications for CR systems where primary and secondary users are geographically distributed and wireless transmissions are subject to path loss and fading.

For a simple illustration, consider a pair of secondary users (A and B) seeking to communicate in the presence of primary users as shown in Fig. 1. A channel is an opportunity to A and B if the transmission from A does not interfere with nearby *primary receivers* in the solid circle, and the reception at B is not affected by nearby *primary transmitters* in the dashed circle. The radius r_I of the solid circle at A, referred to as the interference range of the secondary user, depends on the transmission power of A and the parameter η given by the interference constraint, whereas the radius R_I of the dashed circle (the interference range of primary users) depends on the transmission power of primary users and the interference tolerance of B.

The use of a circle to illustrate the interference region is immaterial. This definition applies to a general signal propagation and interference model by replacing the solid and dashed circles with interference footprints specifying, respectively, the subset of primary receivers who are potential victims of A's transmission and the subset of primary transmitters who can interfere with the reception at B. The key message is that spectrum opportunities depend on both transmitting and receiving activities of primary users. Spectrum opportunity is thus a function of (i) the transmission powers of both primary and secondary users, (ii) the geographical locations of these users, and (iii) the interference constraint. Notice also that

[1]Here we use channel in a general sense: it represents a signal dimension (time, frequency, code, etc.) that can be allocated to a particular user.

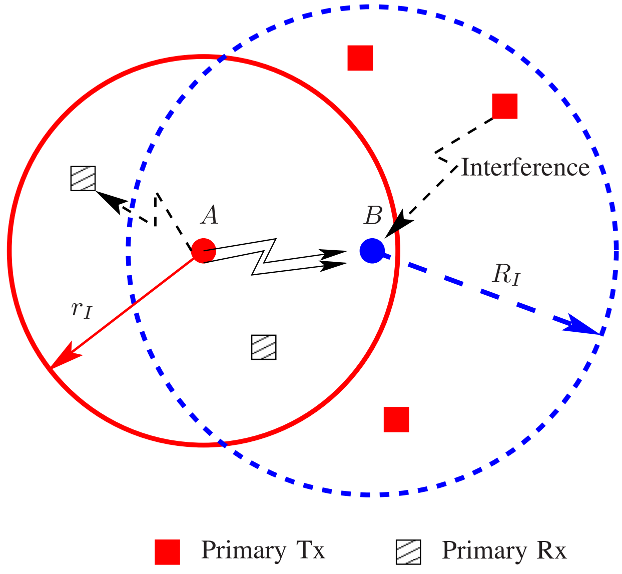

Fig. 1. Illustration of spectrum opportunity (secondary user A wishes to transmit to secondary user B, where A should watch for nearby primary receivers and B nearby primary transmitters).

spectrum opportunities are *asymmetric*. A channel that is an opportunity when A is the transmitter and B the receiver may not be an opportunity when B is the transmitter and A the receiver. This asymmetry leads to a complex dependency of the optimal transmission power on the application type and the use of MAC handshake signaling such as RTS/CTS as shown in Sec. IV and Sec. V.

It is clear from the definition of spectrum opportunity that a higher transmission power (larger r_I in Fig. 1) of the secondary user requires the absence of active primary receivers over a larger area, which occurs less often. The impact of transmission power on the occurrence of opportunity thus follows directly.

B. Impact on the Performance of Opportunity Detection

Spectrum opportunity detection can be considered as a binary hypothesis test. We adopt here the disk signal propagation and interference model as illustrated in Fig. 1. The basic concepts presented here, however, apply to a general model.

Let $\mathbb{I}(A, d, \mathrm{rx})$ denote the logic condition that there exist primary receivers within distance d of the secondary user A. Let $\overline{\mathbb{I}(A, d, \mathrm{rx})}$ denote the complement of $\mathbb{I}(A, d, \mathrm{rx})$. The two hypotheses for opportunity detection are then given by

$$\begin{aligned} \mathcal{H}_0 \quad &: \quad \text{opportunity}, i.e., \overline{\mathbb{I}(A, r_I, \mathrm{rx})} \cap \overline{\mathbb{I}(B, R_I, \mathrm{tx})}, \\ \mathcal{H}_1 \quad &: \quad \text{no opportunity}, i.e., \mathbb{I}(A, r_I, \mathrm{rx}) \cup \mathbb{I}(B, R_I, \mathrm{tx}), \end{aligned}$$

where $\mathbb{I}(B, R_I, \mathrm{tx})$ and $\overline{\mathbb{I}(B, R_I, \mathrm{tx})}$ are similarly defined, and R_I and r_I are, respectively, the interference range of primary and secondary users under the disk model. Notice that $\overline{\mathbb{I}(A, r_I, \mathrm{rx})}$ corresponds to the logic condition on the transmission from A being "harmless", and $\overline{\mathbb{I}(B, R_I, \mathrm{tx})}$ the logic condition on the reception at B being successful.

Detection performance is measured by the probabilities of false alarm P_F and miss detection P_{MD}:

$$\begin{aligned} P_F \quad &= \quad \Pr\{\text{decides } \mathcal{H}_1 \mid \mathcal{H}_0\}, \\ P_{MD} \quad &= \quad \Pr\{\text{decides } \mathcal{H}_0 \mid \mathcal{H}_1\}. \end{aligned}$$

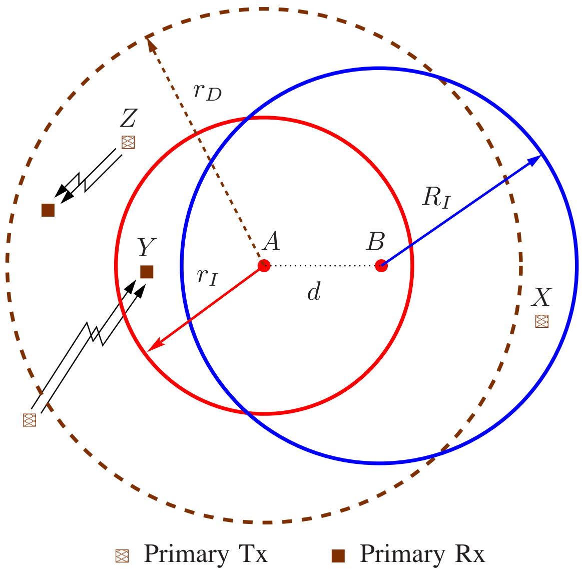

Fig. 2. Spectrum opportunity detection: a common approach that detects spectrum opportunities by observing primary signals (the exposed transmitter Z is a source of false alarms whereas the hidden transmitter X and the hidden receiver Y are sources of miss detections).

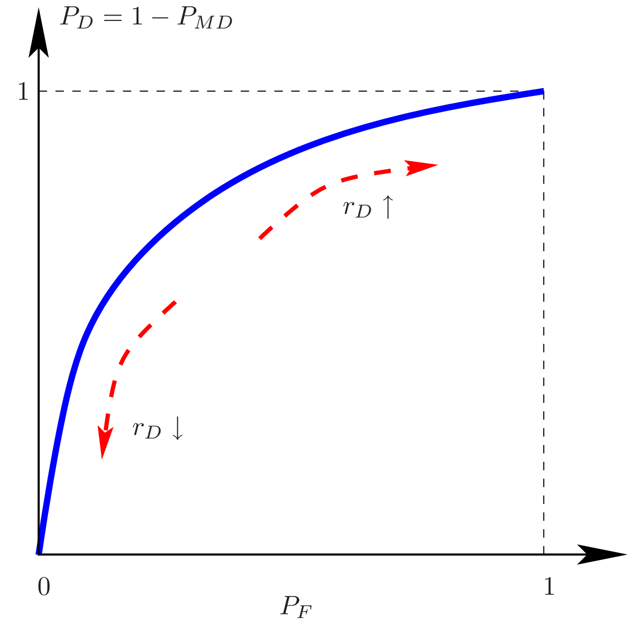

Fig. 3. ROC curve of LBT with a perfect ear (the ROC curve is obtained by varying the detection range r_D).

The tradeoff between false alarm and miss detection is captured by the receiver operating characteristic (ROC) curve, which gives $P_D = 1 - P_{MD}$ (probability of detection or detection power) as a function of P_F. In general, reducing P_F comes at the price of increased P_{MD} and *vice versa*. Since false alarms lead to overlooked spectrum opportunities and miss detections are likely to result in collisions with primary users, the tradeoff between false alarm and miss detection is crucial in the design of CR systems in terms of throughput vs. interference constraint [13].

Without assuming cooperation from primary users, the observations available to the secondary user for opportunity detection are the signals emitted from primary *transmitters*. This basic approach to opportunity detection is commonly referred to as "listen-before-talk" (LBT). As shown in Fig. 2, A infers the existence of spectrum opportunity from the absence of primary transmitters within its detection range r_D, where r_D can be adjusted by changing, for example, the threshold of an energy detector. The probabilities of false alarm P_F and miss detection P_{MD} for LBT are thus given by

$$P_F = \Pr\{\mathbb{I}(A, r_D, \text{tx}) \mid \mathcal{H}_0\}, \quad (1)$$
$$P_{MD} = \Pr\{\overline{\mathbb{I}(A, r_D, \text{tx})} \mid \mathcal{H}_1\}. \quad (2)$$

Uncertainties, however, are inherent to such a scheme even if A listens to primary signals with a perfect ear ($i.e.$, perfect detection of primary transmitters within its detection range r_D). Even in the absence of noise and fading, the geographic distribution and traffic pattern of primary users have significant impact on the performance of LBT. Specifically, there are three possible sources of detection errors: hidden transmitters, hidden receivers, and exposed transmitters. A *hidden transmitter* is a primary transmitter that is located within distance R_I of B but outside the detection range of A (node X in Fig. 2). A *hidden receiver* is a primary receiver that is located within the interference range r_I of A but its corresponding primary transmitter is outside the detection range of A (node Y in Fig. 2). An *exposed transmitter* is a primary transmitter that is located within the detection range of A but transmits to a primary receiver outside the interference range of A (node Z in Fig. 2). For the scenarios shown in Fig. 2, even if A can perfectly detect the presence of signals from any primary transmitters located within its detection range r_D, the transmission from the exposed transmitter Z is a source of false alarms, whereas the transmission from the hidden transmitter X and the reception at the hidden receiver Y are sources of miss detections. It is obvious from (1, 2) that P_F increases but P_{MD} decreases as r_D increases. This tradeoff is captured by the ROC curve. As illustrated in Fig. 3, adjusting the detection range r_D leads to different points on the ROC curve.

From the definition of spectrum opportunity, when $\frac{p_{tx}}{P_{tx}}$ is small (small $\frac{r_I}{R_I}$ in Fig. 1), the occurrence of spectrum opportunity is mainly determined by the logic condition on the reception at B being successful. In this case, errors in detecting opportunity are mainly caused by hidden transmitters such as X in Fig. 2. Since the distance between A and B is relatively small due to the small transmission power, A can accurately infer the presence of primary transmitters in the neighborhood of B, *i.e.*, hidden transmitters are rare, leading to reliable opportunity detection. On the other hand, when $\frac{p_{tx}}{P_{tx}}$ is large (large $\frac{r_I}{R_I}$ in Fig. 1), the occurrence of spectrum opportunity is mainly determined by the logic condition on the transmission from A being "harmless". Due to the relatively small transmission power of the primary users, primary receivers are close to their corresponding transmitters. Node A can thus accurately infer the presence of primary receivers from the presence of primary transmitters and achieve reliable opportunity detection.

To summarize, in the two extreme regimes of $\frac{p_{tx}}{P_{tx}}$, the two logic conditions for spectrum opportunity reduce to one. As a consequence, reducing P_F does not necessarily increase P_{MD}, and perfect spectrum opportunity detection is achieved. A detailed proof of this statement is given in Sec. III-C. Note that we focus on detection errors caused by the inherent uncertainties associated with detecting spectrum opportunities by detecting primary transmitters. Such uncertainties vary with the transmission power of the primary and secondary users. We ignore noise and fading that may cause errors in detecting primary transmitters, since they are not pertinent to the issue of power control for secondary users.

III. Impact of Transmission Power: Quantitative Characterization

In this section, we quantitatively characterize the impact of the transmission power p_{tx} of secondary users by deriving closed-form expressions for the probability of opportunity and the performance of opportunity detection as functions of p_{tx} in a Poisson primary network. The exponential decay of the probability of opportunity with respect to $p_{tx}^{2/\alpha}$ and the asymptotic behavior of the ROC curve are established based on these closed-form expressions.

A. A Poisson Random Network Model

Consider a decentralized primary network, where primary users are distributed according to a two-dimensional homogeneous Poisson process with density λ. At the beginning of each slot, each primary user has a probability p to transmit. For each primary transmitter, its receiver is located uniformly within its transmission range R_p. In the following analysis, we will frequently use the following two classic results on Poisson processes.

Fact 1: Coloring Theorem [14, Chapter 5]
Let Π be a potentially inhomogeneous Poisson process on $\mathbb{R}^d$ with density function $\lambda(\mathbf{x})$, where $\mathbf{x} = (x_1, x_2, ..., x_d) \in \mathbb{R}^d$. Suppose that we obtain Π' by independently coloring points $\mathbf{x} \in \Pi$ according to probabilities $p(\mathbf{x})$. Then Π' and $\Pi - \Pi'$ are two independent Poisson processes with density functions $p(\mathbf{x})\lambda(\mathbf{x})$ and $(1 - p(\mathbf{x}))\lambda(\mathbf{x})$, respectively.

Fact 2: Displacement Theorem [14, Chapter 5]
Let Π be a Poisson process on $\mathbb{R}^d$ with density function $\lambda(\mathbf{x})$. Suppose that the points of Π are displaced randomly and independently. Let $\rho(\mathbf{x}, \mathbf{y})$ denote the probability density of the displaced position $\mathbf{y}$ of a point $\mathbf{x}$ in Π. Then the displaced points form a Poisson process Π' with density function λ' given by $\lambda'(\mathbf{y}) = \int_{\mathbb{R}^d} \lambda(\mathbf{x})\rho(\mathbf{x}, \mathbf{y})\, \mathrm{d}\mathbf{x}$. In particular, if $\lambda(\mathbf{x})$ is a constant λ and $\rho(\mathbf{x}, \mathbf{y})$ is a function of $\mathbf{y} - \mathbf{x}$, then $\lambda'(\mathbf{y}) = \lambda$ for all $\mathbf{y} \in \mathbb{R}^d$.

Note that in the coloring theorem, the original Poisson process Π does not have to be homogeneous and the coloring probability $p(\mathbf{x})$ can depend on the location $\mathbf{x}$. This theorem is more general than the commonly known thinning theorem for homogeneous Poisson processes. In our subsequent analysis, we rely on this general version of the thinning theorem to handle location-dependent coloring.

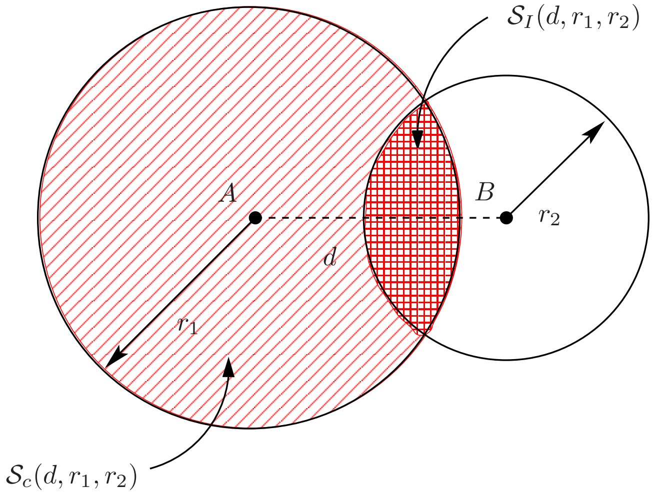

Fig. 4. Illustration of $\mathcal{S}_I(d, r_1, r_2)$ (the common area of two circles with radius r_1 and r_2 and centered d apart) and $\mathcal{S}_c(d, r_1, r_2)$ (the area within a circle with radius r_1 centered at A but outside the circle with radius r_2 centered at B which is distance d away from A).

Based on Fact 1 and Fact 2, we arrive at the following property.

Property 1: Both the primary transmitters and the receivers form a homogeneous Poisson process with density $p\lambda$.
Note that although the two Poisson processes have the same density, they are not independent. We have ignored the case when there is no primary user within the transmission range of a selected primary transmitter. An equivalent primary network model is to start with a two-dimensional homogeneous Poisson process with density $p\lambda$ for primary transmitters, and then for each primary transmitter, place its receiver uniformly within its transmission range R_p.

B. Impact on Probability of Opportunity

Let d be the distance between A and B. Let $\mathcal{S}_I(d, r_1, r_2)$ denote the common area of two circles centered at A and B with radii r_1 and r_2, respectively, and $\mathcal{S}_c(d, r_1, r_2)$ denote the area within a circle with radius r_1 centered at A but outside the circle with radius r_2 centered at B (see Fig. 4). We have the following proposition.

Proposition 1: Probability of Opportunity
Under the disk signal propagation and interference model characterized by $\{r_I, R_I\}$, the probability of opportunity for a pair of secondary users A and B in a Poisson primary network with density λ and traffic load p is given in (3), where the secondary transmitter A is chosen as the origin of the polar coordinate system for the double integral, and d is the distance between A and B.

$$\Pr[\mathcal{H}_0] = \exp\left[-p\lambda\left(\iint\limits_{\mathcal{S}_c(d, r_I+R_p, R_I)} \frac{\mathcal{S}_I(r, R_p, r_I)}{\pi R_p^2} r\mathrm{d}r\mathrm{d}\theta + \pi R_I^2\right)\right]. \tag{3}$$

Proof: Based on the definition of spectrum opportunity, we have

$$\begin{aligned}\Pr[\mathcal{H}_0] &= \Pr\{\overline{\mathbb{I}(A, r_I, \text{rx})} \cap \overline{\mathbb{I}(B, R_I, \text{tx})}\}, \quad (4)\\ &= \Pr\{\overline{\mathbb{I}(A, r_I, \text{rx})} \mid \overline{\mathbb{I}(B, R_I, \text{tx})}\} \Pr\{\overline{\mathbb{I}(B, R_I, \text{tx})}\}.\end{aligned}$$

Based on Property 1, $\Pr\{\overline{\mathbb{I}(B, R_I, \text{tx})}\}$ is given by

$$\Pr\{\overline{\mathbb{I}(B, R_I, \text{tx})}\} = \exp(-p\lambda\pi R_I^2). \quad (5)$$

Next we obtain the first term $\Pr\{\overline{\mathbb{I}(A, r_I, \text{rx})} \mid \overline{\mathbb{I}(B, R_I, \text{tx})}\}$ of (4) based on Fact 1 with location-dependent coloring.

Let Π_{tx} denote the Poisson process formed by the primary transmitters. If we color those primary transmitters in Π_{tx} whose receivers are within distance r_I of A, then from Fact 1 we obtain another Poisson process Π'_{tx} formed by all the colored primary transmitters with density $p\lambda\frac{\mathcal{S}_I(r,R_p,r_I)}{\pi R_p^2}$, where $\frac{\mathcal{S}_I(r,R_p,r_I)}{\pi R_p^2}$ is the coloring probability for a primary transmitter at distance r of A.

Given $\overline{\mathbb{I}(B, R_I, \text{tx})}$, *i.e.*, there are no primary transmitters within distance R_I of B, those primary receivers within distance r_I of A can only communicate with those primary transmitters inside $\mathcal{S}_c(d, r_I + R_p, R_I)$. Thus, the event $\overline{\mathbb{I}(A, r_I, \text{rx})}$ (conditioned on $\overline{\mathbb{I}(B, R_I, \text{tx})}$) occurs if and only if Π'_{tx} does not have any points inside $\mathcal{S}_c(d, r_I + R_p, R_I)$, which immediately leads to (6). Then by substituting (5, 6) into (4), we arrive at (3). ■

While the closed-form expression for $\Pr[\mathcal{H}_0]$ given in (3) appears to be complex with a double integral, it has a simple structure that allows us to establish the monotonicity and the exponential decay rate of $\Pr[\mathcal{H}_0]$ with respect to r_I^2 as given in Theorem 1. Furthermore, as shown in Appendix A, by integrating with respect to θ first, we can reduce the double integral in (3) to a single integral $\int_0^{r_I+R_p} \frac{\mathcal{S}_I(r,R_p,r_I)}{\pi R_p^2} r\theta_0(r)\,\mathrm{d}r$, where $\theta_0(r)$ is a function of the radial coordinate r and is determined by the shape of $\mathcal{S}_c(d, r_I + R_p, R_I)$. The basic idea is that the integrand in (3) is not a function of the angular coordinate θ and the range of θ as a function of the radial coordinate r can be obtained in an explicit form. In the integrand of the obtained single integral, $\mathcal{S}_I(r, R_p, r_I)$ that depends on r is also in an explicit form as obtained in [15] and provided in Appendix A. As a consequence, the resulting single integral is easy to compute.

From (3), we arrive at the following theorem that characterizes the impact of the transmission power p_{tx} on the probability of opportunity.

Theorem 1: Impact on Opportunity Occurrence

T1.1. $\Pr[\mathcal{H}_0]$ is a strictly decreasing function of $p_{tx} \propto r_I^{\alpha}$.

T1.2. $\Pr[\mathcal{H}_0]$ decreases exponentially[2] with $p_{tx}^{2/\alpha} \propto r_I^2$, where the decay constant is proportional to $p\lambda$, *i.e.*, $\exp(-p\lambda\pi R_I^2) < \frac{\Pr[\mathcal{H}_0]}{\exp(-p\lambda\pi r_I^2)} \leq 1$, with equality when $r_I \geq d + R_I + R_p$.

T1.3. $\Pr[\mathcal{H}_0]$ decreases exponentially with $p\lambda$, where the decay constant is $\pi r_I^2 \propto p_{tx}^{2/\alpha}$.

Proof: Theorem 1 is obtained by examining the closed-form expression for $\Pr[\mathcal{H}_0]$ given in (3). Details are given in Appendix B. ■

From T1.2, we can see that when the transmission power of secondary users is high ($r_I \geq d + R_I + R_p$), the probability of opportunity $\Pr[\mathcal{H}_0]$ has a simple expression: $\Pr[\mathcal{H}_0] = \exp(-p\lambda\pi r_I^2)$. When $r_I \geq d+R_I+R_p$, the absence of primary receivers within distance r_I of A automatically implies the absence of primary transmitters within distance R_I of B. Thus, the opportunity occurs if and only if there is no primary receiver within distance r_I of A, which leads to the simple expression for $\Pr[\mathcal{H}_0]$. Moreover, from T1.2 we can see that the traffic load $p\lambda$ of primary users determines the exponential decay rate of $\Pr[\mathcal{H}_0]$ with respect to $p_{tx}^{2/\alpha}$. Similarly, T1.3 shows that the area πr_I^2 "consumed" by the secondary transmitter, a concept introduced in [4], is the decay constant of $\Pr[\mathcal{H}_0]$ with respect to $p\lambda$.

A numerical example is given in Fig. 5(a), where $\Pr[\mathcal{H}_0]$ and its lower and upper bounds ($\exp[-p\lambda\pi(r_I^2 + R_I^2)]$ and $\exp(-p\lambda\pi r_I^2)$, respectively) given in T1.2 are plotted as a function of r_I. The exponential decay rate of $\Pr[\mathcal{H}_0]$ can be easily observed by noticing the log scale. Fig. 5(b) depicts $\Pr[\mathcal{H}_0]$ as a function of $p\lambda$ for different r_I. It shows that the exponential decay constant of $\Pr[\mathcal{H}_0]$ with respect to $p\lambda$ increases as r_I increases.

C. Impact on Detection Performance

In the following, we focus on the performance of the spectrum opportunity detector for one pair of secondary users A and B, where there are no other secondary users in the network.

For LBT, false alarms occur if and only if there exist primary transmitters within the detection range r_D of A under $\mathcal{H}_0$, and miss detections occur if and only if there is no primary transmitter within the detection range r_D of A under $\mathcal{H}_1$. We thus have the following proposition.

Proposition 2: False Alarm and Miss Detection Probabilities

Under the disk model characterized by $\{r_I, R_I\}$, let r_D be the detection range. The probabilities of false alarm P_F and miss detection P_{MD} for a pair of secondary users A and B in a Poisson primary network with density λ and traffic load p are given in (7, 8), where the secondary transmitter A is chosen as the origin of the polar coordinate system for the double integral, d is the distance between A and B, and $\mathcal{S}_o = \mathcal{S}_c(d, r_D, R_I) \cap \mathcal{S}_c(d, r_I + R_p, R_I)$.

Proof: Similar to Proposition 1, the proof uses Fact 1 with location-dependent coloring. For details, see Appendix C. ■

[2]A quantity N is said to decrease exponentially with respect to t if its decay rate is proportional to its value. Symbolically, this can be expressed as the following differential equation: $\frac{\mathrm{d}N}{\mathrm{d}t} = -\lambda N$, where $\lambda > 0$ is called the decay constant.

$$\Pr\{\overline{\mathbb{I}(A, r_I, \text{rx})} \mid \overline{\mathbb{I}(B, R_I, \text{tx})}\} = \exp\left(-\iint_{\mathcal{S}_c(d,r_I+R_p,R_I)} p\lambda\frac{\mathcal{S}_I(r, R_p, r_I)}{\pi R_p^2} r\mathrm{d}r\mathrm{d}\theta\right). \quad (6)$$

$$P_F = 1-\exp\left[-p\lambda\left(\pi r_D^2 - \mathcal{S}_I(d,r_D,R_I) - \iint_{\mathcal{S}_o}\frac{\mathcal{S}_I(r,R_p,r_I)}{\pi R_p^2}\mathrm{r}\mathrm{d}\mathrm{r}\mathrm{d}\theta\right)\right], \tag{7}$$

$$P_{MD} = \frac{\exp(-p\lambda\pi r_D^2) - \exp\left[-p\lambda\left(\pi(r_D^2+R_I^2) - \mathcal{S}_I(d,r_D,R_I) + \iint_{\mathcal{S}_c(d,r_I+R_p,R_I)-\mathcal{S}_o}\frac{\mathcal{S}_I(r,R_p,r_I)}{\pi R_p^2}\mathrm{r}\mathrm{d}\mathrm{r}\mathrm{d}\theta\right)\right]}{1-\exp\left[-p\lambda\left(\iint_{\mathcal{S}_c(d,r_I+R_p,R_I)}\frac{\mathcal{S}_I(r,R_p,r_I)}{\pi R_p^2}\mathrm{r}\mathrm{d}\mathrm{r}\mathrm{d}\theta + \pi R_I^2\right)\right]}. \tag{8}$$

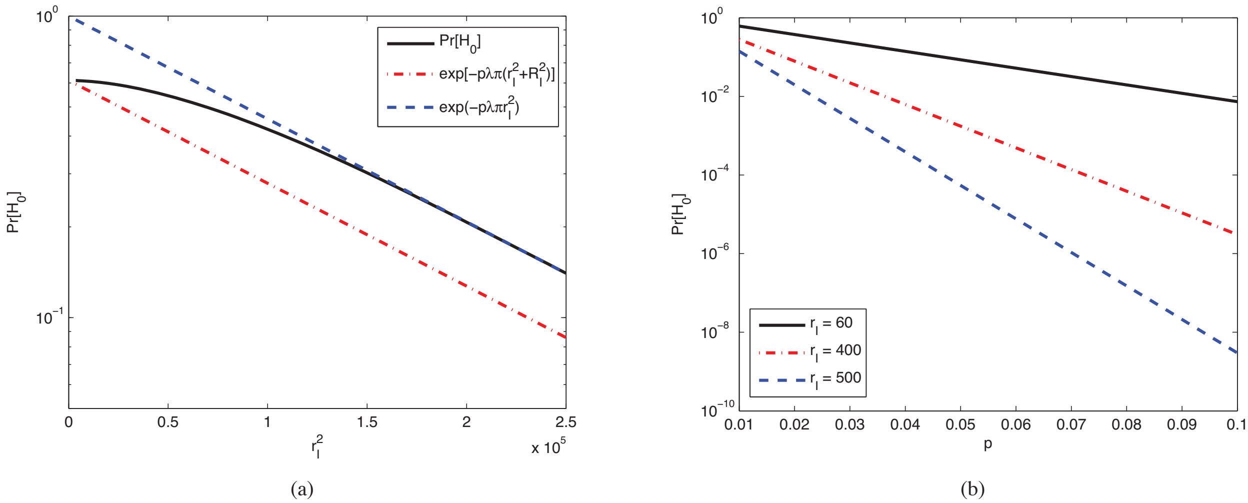

Fig. 5. (a) $\Pr[\mathcal{H}_0]$ vs r_I ($p = 0.01$, $\lambda = 10/200^2$, $d = 50$, $R_p = 200$, $R_I = 250$); (b) $\Pr[\mathcal{H}_0]$ vs p ($\lambda = 10/200^2$, $d = 50$, $R_p = 200$, $R_I = 250$). Note that both y-axes use log-scale.

Similar to (3), the double integral in (7, 8) can be simplified to a single integral due to the independence of the integrand with respect to the angular coordinate θ and the special shape of $\mathcal{S}_o$. Due to the page limit, we omit the details which may be found in [16].

From Proposition 2, we can show the following theorem that characterizes the impact of the transmission power of secondary users (represented by r_I) on the asymptotic behavior of the ROC curve for spectrum opportunity detection.

Theorem 2: Impact on Detection Performance[3]. There exist two points on the ROC curve that asymptotically approach $(0,1)$ as $\frac{r_I}{R_I} \to 0$ and ∞, respectively. Specifically,

$$\lim_{\frac{r_I}{R_I}\to 0}(P_F,P_D) = (0,1), \text{ for } r_D = R_I;$$

$$\lim_{\frac{r_I}{R_I}\to \infty}(P_F,P_D) = (0,1), \text{ for } r_D = r_I - R_I.$$

Proof: The intuitive reasons for choosing $r_D = R_I$ and $r_D = r_I - R_I$ in the two extreme regimes are discussed in Sec. II-B. For details of the proof, see Appendix D. ■

Since $(0,1)$ is the perfect operating point on a ROC curve, we can asymptotically approach perfect detection performance by choosing $r_D = R_I$ when $\frac{r_I}{R_I} \to 0$ or $r_D = r_I - R_I$ when $\frac{r_I}{R_I} \to \infty$. A numerical example is shown in Fig. 6, where the ROC curve approaches the corner $(0,1)$ as $\frac{r_I}{R_I}$ increases or decreases.

[3]Since the minimum transmission power for successful reception is, in general, higher than the maximum allowable interference power, it follows that the transmission range R_p of primary users is smaller than R_I. Furthermore, under the disk signal propagation and interference model, we have $R_p = \beta R_I$ $(0 < \beta < 1)$. A similar relationship holds for d and r_I.

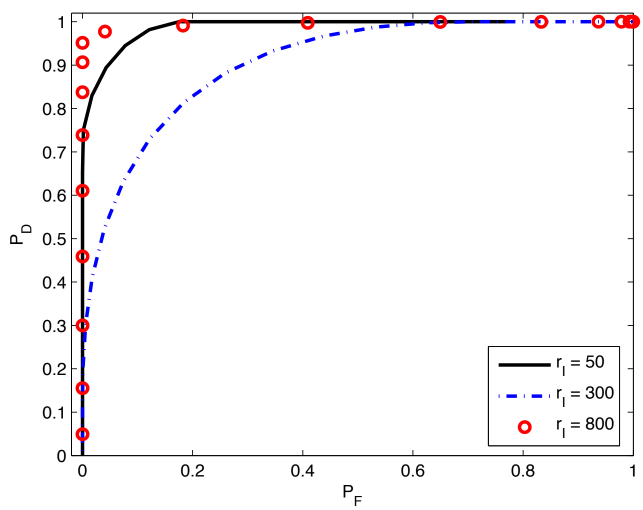

Fig. 6. ROC curve for LBT ($p = 0.01$, $\lambda = 10/200^2$, $R_p = 200$, $R_I = R_p/0.8 = 250$, $d = 0.9r_I$)

IV. Power Control for Optimal Transport Throughput

In this section, the impacts of the transmission power on the occurrence of opportunities and the reliability of opportunity detection are integrated together for optimal power control. Under the performance measure of transport throughput subject to an interference constraint, we examine how a secondary user should choose its transmission power according to the interference constraint, the traffic load and transmission power of primary users, and its own application type (guaranteed delivery vs. best-effort delivery).

A. Transport Throughput

From Sec. III-B and Sec. III-C, it seems that the transmission power p_{tx} should be chosen as small as possible to maximize the probability of opportunity and improve detection quality. Such a choice of the transmission power, however, does not lead to an efficient communication system due to the small distance covered by the transmission. We adopt here transport throughput as the performance measure, which is defined as

$$C(r_I, r_D) = d(r_I) P_S(r_D, r_I), \tag{9}$$

where $d(\propto r_I)$ is the transmission range of the secondary user, and P_S is the probability of successful data transmission which depends on both the occurrence of opportunities and the reliability of opportunity detection. Then power control for optimal transport throughput can be formulated as a constrained optimization problem:

$$r_I^* = \arg\max_{r_I}\{C\} = \arg\max_{r_I}\{d(r_I)P_S(r_D, r_I)\}, \tag{10}$$
$$\text{s.t. } P_C(r_D, r_I) \leq \zeta,$$

where ζ is the maximum allowable collision probability given by the interference constraint, P_C the probability of colliding with primary users which depends on the reliability of opportunity detection. Note that the detection range r_D is not an independent parameter; it is determined by maximizing $P_S(r_D, r_I)$ subject to $P_C(r_D, r_I) \leq \zeta$ for a given interference range r_I.

In order to solve the above constrained optimization problem, we need expressions for P_C and P_S which collectively measure the MAC layer performance.

B. MAC Performance of LBT

We first consider P_S, which is application dependent. For applications requiring guaranteed delivery, an acknowledgement (ACK) signal from the secondary receiver B to the secondary transmitter A is required to complete a data transmission. Specifically, in a successful data transmission, the following three events should occur in sequence: A detects the opportunity ($\overline{\mathbb{I}(A, r_D, \text{tx})}$) and transmits data to B; B receives data successfully ($\overline{\mathbb{I}(B, R_I, \text{tx})}$) and replies to A with an ACK[4]; A receives the ACK ($\overline{\mathbb{I}(A, R_I, \text{tx})}$) which completes the transmission. We thus have

$$\begin{aligned} P_S &= \Pr\{\overline{\mathbb{I}(A, r_D, \text{tx})} \cap \overline{\mathbb{I}(B, R_I, \text{tx})} \cap \overline{\mathbb{I}(A, R_I, \text{tx})}\}, \\ &= \Pr\{\overline{\mathbb{I}(A, r_E, \text{tx})} \cap \overline{\mathbb{I}(B, R_I, \text{tx})}\}, \end{aligned} \tag{11}$$

where $r_E = \max\{r_D, R_I\}$ is referred to as the effective detection range.

For best-effort delivery applications [17], acknowledgements are not required to confirm the completion of data transmissions. In this case, we have

$$P_S = \Pr\{\overline{\mathbb{I}(A, r_D, \text{tx})} \cap \overline{\mathbb{I}(B, R_I, \text{tx})}\}. \tag{12}$$

The probability of collision is defined as

$$P_C = \Pr\{A \text{ transmits data} \mid \mathbb{I}(A, r_I, \text{rx})\}. \tag{13}$$

Note that P_C is conditioned on $\mathbb{I}(A, r_I, \text{rx})$ instead of $\mathcal{H}_1$. Clearly, $\Pr[\mathbb{I}(A, r_I, \text{rx})] \leq \Pr[\mathcal{H}_1]$.

Since the secondary transmitter A transmits data if and only if A detects no nearby primary transmitters, we thus have

$$P_C = \Pr\{\overline{\mathbb{I}(A, r_D, \text{tx})} \mid \mathbb{I}(A, r_I, \text{rx})\}. \tag{14}$$

By considering the Poisson primary network and the disk interference model, we obtain the closed-form expressions for P_C and P_S given in the following proposition.

Proposition 3: Collision and Successful Probabilities Under the disk model characterized by $\{r_I, R_I\}$, let r_D be the detection range. The probabilities of collision P_C and successful transmission P_S for a pair of secondary users A and B in a Poisson primary network with density λ and traffic load p are given in (15, 16).

Proof: Similar to Proposition 2, the derivation of P_C uses Fact 1 with location-dependent coloring. For details, see Appendix E. The expressions for P_S follow immediately from (11, 12) and Property 1. ■

Based on the expression for $\mathcal{S}_I(r, r_I, R_p)$, we can obtain $I(r_D, r_I, R_p)$ in an explicit form without integral. Details are left in [16] due to the page limit. Notice that the above expressions for P_C and P_S are in explicit form without integrals. With the explicit expressions for P_C (15) and P_S (16), the constrained optimization given in (10) can be solved numerically.

C. Numerical Examples

Shown in Fig. 7 is a numerical example where we plot transport throughput C as a function of r_I. Notice that r_I^* is the interference range for optimal transport throughput. We can see that r_I^* for best-effort applications is different from that for guaranteed delivery, and neither of them is in the two extreme regimes. We also observe that the optimal transport throughput for best-effort delivery is larger than that for guaranteed delivery. This example thus demonstrates that OSA based on cognitive radio is more suitable for best-effort applications as compared to guaranteed delivery due to the asymmetry of spectrum opportunities.

Fig. 8 shows how the optimal transmission power of the secondary user varies with the traffic load and transmission power of the primary users, as well as the application type of the secondary user. Specifically, the optimal interference range r_I^* decreases as the traffic load increases. This agrees

[4]We assume that the interference to primary users caused by an ACK signal is negligible due to its short duration. B thus transmits an ACK signal whenever it receives a data packet successfully.

$$P_C = \frac{\exp(-p\lambda\pi r_D^2)[1-\exp(-p\lambda\pi(r_I^2 - I(r_D, r_I, R_p)))]}{1-\exp(-p\lambda\pi r_I^2)}, \quad (15)$$

$$P_S = \begin{cases} \exp[-p\lambda(\pi(r_E^2 + R_I^2) - \mathcal{S}_I(d, r_E, R_I))], & \text{for guaranteed delivery,} \\ \exp[-p\lambda(\pi(r_D^2 + R_I^2) - \mathcal{S}_I(d, r_D, R_I))], & \text{for best-effort delivery,} \end{cases} \quad (16)$$

where $I(r_D, r_I, R_p) = \int_0^{r_D} 2r\frac{\mathcal{S}_I(r, r_I, R_p)}{\pi R_p^2}\mathrm{d}r$.

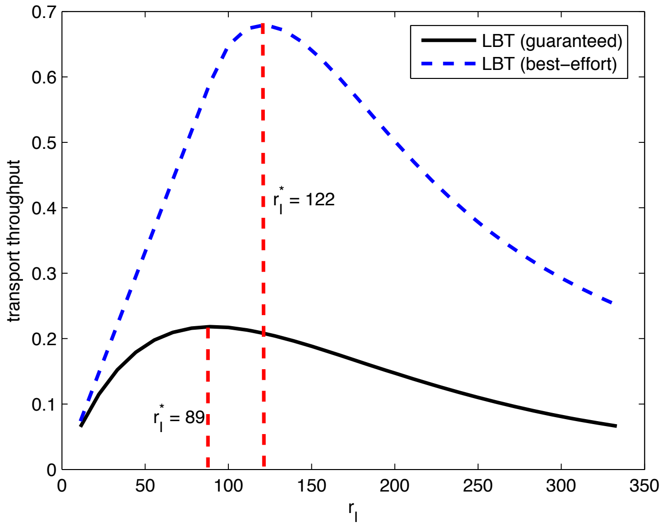

Fig. 7. Transport Throughput vs r_I ($p = 0.1$, $\lambda = 10/200^2$, $R_p = 200$, $R_I = R_p/0.8 = 250$, $d = 0.9r_I$, $\zeta = 0.05$)

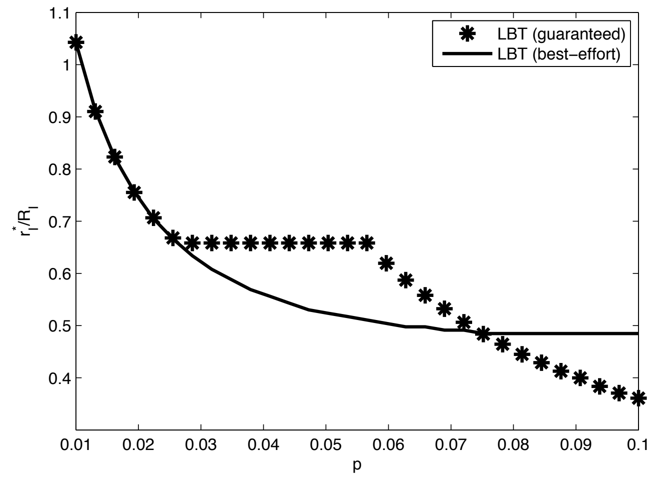

Fig. 8. Ratio between optimal interference range r_I^* for transport throughput and R_I vs traffic load p of primary users ($\lambda = 10/200^2$, $R_p = 200$, $R_I = R_p/0.8 = 250$, $d = 0.9r_I$, $\zeta = 0.05$)

with our intuition from the analogy of crossing a multi-lane highway. Furthermore, the optimal transmission power of the secondary user is related to that of the primary user. We can see from Fig 8 that when the traffic load is low, r_I^* is close to the interference range R_I of primary transmitters. When the traffic load is high, r_I^* is much smaller than R_I.

V. RTS/CTS-Enhanced LBT

The sources of the detection error floor of LBT in the absence of noise and fading resemble the hidden and exposed terminal problem in conventional ad hoc networks of peer users. It is thus natural to consider the use of RTS/CTS handshake signaling to enhance the detection performance of LBT. For RTS/CTS-enhanced LBT (ELBT), spectrum opportunity detection is performed jointly by the secondary transmitter A and the secondary receiver B through the exchange of RTS/CTS signals. The detailed steps are given below.

- A detects primary transmitters within distance r_D. If it detects none, A sends B a Ready-to-Send (RTS) signal.
- If B receives the RTS signal from A successfully, then B replies with a Clear-to-Send (CTS) signal.
- Upon receiving the CTS signal, A transmits to B.

Since for ELBT, the observation space comprises the RTS and CTS signals, we have the following for the probabilities of false alarm P_F and miss detection P_{MD}.

$$\begin{aligned} P_F &= \Pr\{\text{failed RTS/CTS exchange} \mid \mathcal{H}_0\}, \\ &= \Pr\{\mathbb{I}(A, r_D, \text{tx}) \cup \mathbb{I}(B, R_I, \text{tx}) \cup \mathbb{I}(A, R_I, \text{tx}) \mid \mathcal{H}_0\}, \\ &= \Pr\{\mathbb{I}(A, r_E, \text{tx}) \mid \mathcal{H}_0\}, \quad (17) \\ P_{MD} &= \Pr\{\text{successful RTS/CTS exchange} \mid \mathcal{H}_1\}, \\ &= \Pr\{\overline{\mathbb{I}(A, r_D, \text{tx})} \cap \overline{\mathbb{I}(B, R_I, \text{tx})} \cap \overline{\mathbb{I}(A, R_I, \text{tx})} \mid \mathcal{H}_1\}, \\ &= \Pr\{\overline{\mathbb{I}(A, r_E, \text{tx})} \cap \overline{\mathbb{I}(B, R_I, \text{tx})} \mid \mathcal{H}_1\}, \quad (18) \end{aligned}$$

where the last step in obtaining (17) follows from $\Pr\{\mathbb{I}(B, R_I, \text{tx}) \cap \mathcal{H}_0\} = 0$.

Since A transmits data if and only if a successful RTS/CTS exchange occurs, it follows that[5]

$$P_C = \Pr\{\overline{\mathbb{I}(A, r_E, \text{tx})} \cap \overline{\mathbb{I}(B, R_I, \text{tx})} \mid \mathbb{I}(A, r_I, \text{rx})\}. \quad (19)$$

Unlike LBT, miss detections always lead to successful data transmissions for ELBT. This is because miss detections can only occur after a successful RTS-CTS exchange. Then B can receive data successfully as it can receive RTS. We thus have

$$\begin{aligned} P_S &= (1-P_F)\cdot\Pr[\mathcal{H}_0] + P_{MD}\cdot\Pr[\mathcal{H}_1], \\ &= \Pr\{\overline{\mathbb{I}(A, r_E, \text{tx})} \cap \overline{\mathbb{I}(B, R_I, \text{tx})}\}. \quad (20) \end{aligned}$$

Notice that P_S of ELBT is identical to that of LBT for guaranteed delivery in (11). Due to the requirement on the successful reception of CTS in opportunity detection, P_S for

[5]In obtaining the definition (19) of P_C, we have assumed that the interference caused by the RTS, CTS and ACK signals is negligible due to their short durations.

ELBT is independent of the application, *i.e.*, whether or not ACK is required.

Based on (17–20), we obtain the following proposition for the Poisson primary network model.

Proposition 4: PHY and MAC Performance of ELBT Under the disk model characterized by $\{r_I, R_I\}$, let r_D be the detection range. The probabilities of false alarm P_F, miss detection P_{MD}, collision P_C, and successful transmission P_S for a pair of secondary users A and B in a Poisson primary network with density λ and traffic load p are given in (21–24). Furthermore, Theorem 2 also holds for ELBT, *i.e.*, perfect detection performance can be achieved at $r_D = R_I$ when $\frac{r_I}{R_I} \to 0$ and at $r_D = r_I - R_I$ when $\frac{r_I}{R_I} \to \infty$.

Proof: The derivations of the above expressions and the proof of Theorem 2 are very similar to those for LBT. Details are left in [16]. ■

Similarly, based on (23, 24), we can obtain numerical solutions to the constrained optimization problem (10) for ELBT. Fig. 9 shows the maximum transport throughput as a function of the traffic load p obtained by optimizing r_I. We observe from Fig. 9 that RTS/CTS handshake signaling improves the performance of LBT when the traffic load is low, but it degrades the performance of LBT with best-effort delivery when the traffic load is high. This is because asymmetric opportunities that give rise to a unidirectional link from A to B cannot be exploited under ELBT. This suggests that even when the overhead associated with RTS/CTS is ignored, RTS/CTS may lead to performance degradation for best-effort applications. When the traffic load is high, LBT with best-effort delivery gives the best transport throughput. This is consistent with our previous observation obtained from Fig. 7 that best-effort is a more suitable application to be considered for overlaying with a primary network with relatively high traffic load.

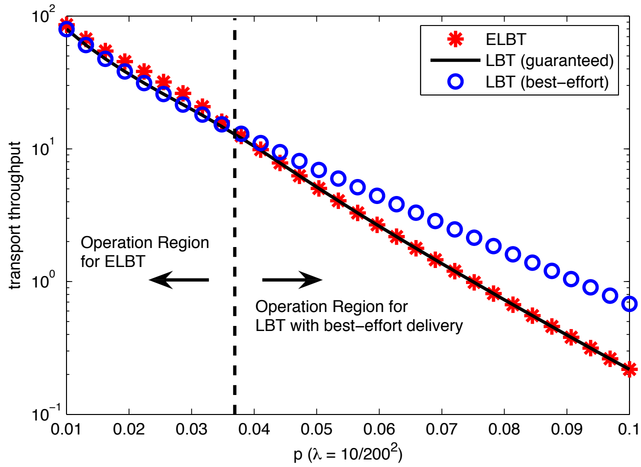

Fig. 9. Transport throughput vs traffic load p of primary users ($\lambda = 10/200^2$, $R_p = 200$, $R_I = R_p/0.8 = 250$, $d = 0.9r_I$, $\zeta = 0.05$)

VI. Conclusion and Discussion

We have studied transmission power control of secondary users in CR networks. By carefully examining the concepts of spectrum opportunity and interference constraint, we have revealed and analytically characterized the impacts of transmission power on the occurrence of spectrum opportunities and the reliability of opportunity detection. Based on a Poisson model of the primary network, we have quantified these impacts by showing the exponential decay rate of the probability of opportunity with respect to the transmission power and the asymptotic behavior of the ROC curve for opportunity detection. Such analytical characterizations allow us to design the transmission power for optimal transport throughput under constraints on the interference to primary users.

Furthermore, the non-equivalence between detecting primary signals and detecting spectrum opportunities has been clarified. It has been demonstrated that besides noise and fading, the geographical distribution and traffic pattern of primary users have significant impact on the performance of physical layer spectrum sensing. The complex dependency of the PHY-MAC interaction on the application types and the use of MAC handshake signaling such as RTS/CTS is also illustrated.

$$P_F = 1 - \exp\left[-p\lambda\left(\pi r_E^2 - \mathcal{S}_I(d, r_E, R_I) - \iint_{\mathcal{S}'_o} \frac{\mathcal{S}_I(r, R_p, r_I)}{\pi R_p^2} r\mathrm{d}r\mathrm{d}\theta\right)\right], \tag{21}$$

$$P_{MD} = \frac{\exp[-p\lambda(\pi(r_E^2 + R_I^2) - \mathcal{S}_I(d, r_E, R_I))]\left[1 - \exp\left(-p\lambda \iint_{\mathcal{S}_c(d, r_I+R_p, R_I) - \mathcal{S}'_o} \frac{\mathcal{S}_I(r,R_p,r_I)}{\pi R_p^2} r\mathrm{d}r\mathrm{d}\theta\right)\right]}{1 - \exp\left[-p\lambda\left(\iint_{\mathcal{S}_c(d, r_I+R_p, R_I)} \frac{\mathcal{S}_I(r,R_p,r_I)}{\pi R_p^2} r\mathrm{d}r\mathrm{d}\theta + \pi R_I^2\right)\right]}, \tag{22}$$

$$P_C = \frac{\exp[-p\lambda(\pi(r_E^2 + R_I^2) - \mathcal{S}_I(d, r_E, R_I))]\left[1 - \exp\left(-p\lambda \iint_{\mathcal{S}_c(d, r_I+R_p, R_I) - \mathcal{S}'_o} \frac{\mathcal{S}_I(r,R_p,r_I)}{\pi R_p^2} r\mathrm{d}r\mathrm{d}\theta\right)\right]}{1 - \exp\left(p\lambda\pi r_I^2\right)}, \tag{23}$$

$$P_S = \exp[-p\lambda(\pi(r_E^2 + R_I^2) - \mathcal{S}_I(d, r_E, R_I))], \tag{24}$$

where $\mathcal{S}'_o = \mathcal{S}_c(d, r_E, R_I) \cap \mathcal{S}_c(d, r_I + R_p, R_I)$.

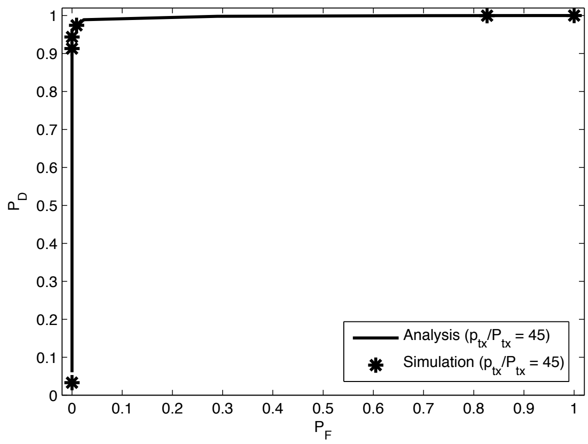

(a)

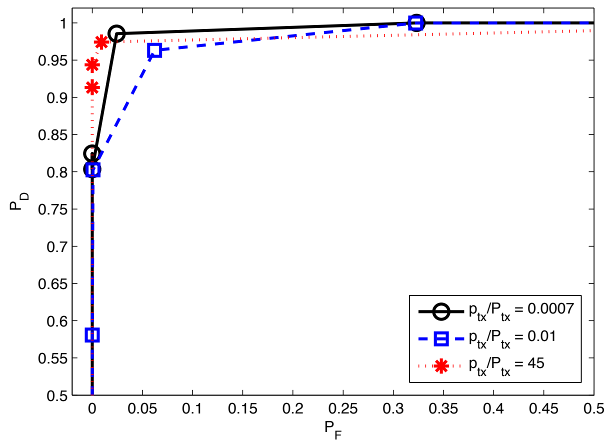

(b)

Fig. 10. (a) Simulated ROC curve of energy detector vs. analytical ROC curve of LBT; (b) Simulated ROC curves of energy detector. Other parameters are given in $p = 0.01$, $\lambda = 10/200^2$, $P_{tx} = 10$, $R_p = 200$, $R_I = R_p/0.8 = 250$, $\tau_B = P_{tx} \cdot R_I^{-\alpha}$, $\alpha = 3$, $r_I = (p_{tx}/\tau_B)^{\frac{1}{\alpha}}$, $d = 0.9 \cdot r_I$.

In the above analysis, the interference region of primary users is represented by a circle with radius R_I. It is possible that the interference contributions from multiple interferers outside this circle cause an outage at the secondary receiver B. By choosing a conservative interference range R_I, however, this possibility is negligible [18]. To verify this, we consider a simulation example where we take into account the accumulated interference power from all primary transmitters. In this case, a channel is an opportunity for a pair of secondary users if there is no primary receiver within the interference range r_I of the secondary transmitter A and the total power of the interference I_B from all primary transmitters to the secondary receiver B is below some prescribed level τ_B, *i.e.*, $\overline{\mathbb{I}(A, r_I, \mathrm{rx})} \cap (I_B < \tau_B)$. To detect a spectrum opportunity, the secondary transmitter A uses an energy detector, which is given by

$$I_A \underset{\mathcal{H}_1}{\overset{\mathcal{H}_0}{\lessgtr}} \tau_A,$$

where I_A is the total received power at the secondary transmitter A and τ_A is the threshold of the energy detector. Let Π_{tx} denote the Poisson point process of primary transmitters, d_i^A and d_i^B the distance from the i^{th} primary transmitter to A and B, respectively, and α the path-loss exponent, then we have

$$I_A = \sum_{i \in \Pi_{tx}} P_{tx} \cdot (d_i^A)^{-\alpha}, \qquad I_B = \sum_{i \in \Pi_{tx}} P_{tx} \cdot (d_i^B)^{-\alpha}.$$

Fig. 10(a) shows the simulated ROC curve of the energy detector, which matches well with the analytical ROC curve of LBT. In Fig. 10(b), we see that reliable opportunity detection can still be achieved by the energy detector when $\frac{p_{tx}}{P_{tx}} \to 0$ and $\frac{p_{tx}}{P_{tx}} \to \infty$. In other words, the asymptotic property of the ROC curve (Theorem 2) still holds in this case.

As an initial analysis, we have focused on a single pair of secondary users. When there are multiple secondary users, our definition of spectrum opportunity still applies, although determining the interference range r_I of secondary users needs careful consideration due to the accumulation of the interference power from multiple secondary transmitters. Considering a Poisson secondary network overlaid with a Poisson primary network, we have studied the connectivity of CR networks in [19] using theories and techniques from continuum percolation. The impact of secondary users' transmission power on the occurrence of spectrum opportunities revealed in this paper has been extended in [19] to address the tradeoff between proximity (the number of neighbors) and opportunity (the number of connected links permitted by spectrum opportunities).

Appendix A: Simplification of the Double Integral in $\Pr[\mathcal{H}_0]$

By considering the shape of $\mathcal{S}_c(d, r_I + R_p, R_I)$ (see [16]), we use the independence of the integrand on the angular coordinate θ to reduce the double integral to a single integral with respect to the radial coordinate r. Here we choose the secondary transmitter A as the origin of the polar coordinate system and the line from the secondary transmitter A to the secondary receiver B as the polar axis. Due to the symmetry of $\mathcal{S}_c(d, r_I + R_p, R_I)$ with respect to the polar axis, there is a coefficient 2 before each integral below. Define

$$\begin{aligned} Q &= \iint\limits_{\mathcal{S}_c(d, r_I + R_p, R_I)} \frac{\mathcal{S}_I(r, R_p, r_I)}{\pi R_p^2} r \mathrm{d}r \mathrm{d}\theta, \\ I(r, R_p, r_I) &= 2 \int_0^r t \frac{\mathcal{S}_I(t, R_p, r_I)}{\pi R_p^2} \mathrm{d}t, \\ \theta_0(r) &= \arccos\left(\frac{d^2 + r^2 - R_I^2}{2dr}\right), \end{aligned}$$

then we have the following two cases.

☐ Case 1: $R_I \geq d$.

- If $r_I + R_p \leq R_I - d$, then $Q = 0$.

- If $R_I - d < r_I + R_p < R_I + d$, then

$$Q = \pi[r_I^2 - I(R_I - d, R_p, r_I)] - 2\int_{R_I-d}^{r_I+R_p} \frac{\mathcal{S}_I(r, R_p, r_I)}{\pi R_p^2} r\theta_0(r)\mathrm{d}r.$$

- If $r_I + R_p > R_I + d$, then

$$Q = \pi[r_I^2 - I(R_I - d, R_p, r_I)] - 2\int_{R_I-d}^{R_I+d} \frac{\mathcal{S}_I(r, R_p, r_I)}{\pi R_p^2} r\theta_0(r)\mathrm{d}r.$$

□ Case 2: $R_I < d$.

- If $r_I + R_p \leq d - R_I$, then $Q = \pi r_I^2$.
- If $d - R_I < r_I + R_p < d + R_I$, then $Q = \pi r_I^2 - 2\int_{d-R_I}^{r_I+R_p} \frac{\mathcal{S}_I(r,R_p,r_I)}{\pi R_p^2} r\theta_0(r)\mathrm{d}r$.
- If $r_I + R_p > d + R_I$, then $Q = \pi r_I^2 - 2\int_{d-R_I}^{d+R_I} \frac{\mathcal{S}_I(r,R_p,r_I)}{\pi R_p^2} r\theta_0(r)\mathrm{d}r$.

The expression for $I(r, R_p, r_I)$ is obtained in an explicit form as listed below.

□ Case 1: for $r \leq |R_p - r_I|$,

$$I(r, R_p, r_I) = r^2 \min\left\{1, \frac{r_I^2}{R_p^2}\right\}.$$

□ Case 2: for $|R_p - r_I| < r < R_p + r_I$, $I(r, R_p, r_I)$ is given in (A1).

□ Case 3: for $r \geq R_p + r_I$, $I(r, R_p, r_I) = r_I^2$.

To compute the remaining integral $\int \frac{\mathcal{S}_I(r,R_p,r_I)}{\pi R_p^2} r\theta_0(r)\mathrm{d}r$ numerically, we need an explicit-form expression for $\mathcal{S}_I(r, R_p, r_I)$, which is given by

□ Case 1: for $0 \leq r \leq |R_p - r_I|$,

$$\mathcal{S}_I(r, R_p, r_I) = \pi \min\{R_p^2, r_I^2\}.$$

□ Case 2 [15]: for $|R_p - r_I| < r < R_p + r_I$,

$$\mathcal{S}_I(r, R_p, r_I) = R_p^2 \arccos\left(\frac{R_p^2 + r^2 - r_I^2}{2R_p r}\right) + r_I^2 \arccos\left(\frac{r_I^2 + r^2 - R_p^2}{2r_I r}\right) - r\sqrt{r_I^2 - \left(\frac{r_I^2 + r^2 - R_p^2}{2r}\right)^2}.$$

□ Case 3: for $r \geq R_p + r_I$, $\mathcal{S}_I(r, R_p, r_I) = 0$.

Appendix B: Proof of Theorem 1

Since the integrand $\frac{\mathcal{S}_I(r,R_p,r_I)}{\pi R_p^2}$ and the region of the double integral $\mathcal{S}_c(d, r_I + R_p, R_I)$ are both increasing functions of r_I [16], T1.1 follows from the monotonicity of the exponential function. Similarly, T1.3 follows from the monotonicity of the exponential function.

We now prove T1.2. Recall the definition of opportunity,

$$\begin{aligned}\Pr[\mathcal{H}_0] &= \Pr\{\overline{\mathbb{I}(A, r_I, \mathrm{rx})} \cap \overline{\mathbb{I}(B, R_I, \mathrm{tx})}\} \\ &= \Pr\{\overline{\mathbb{I}(A, r_I, \mathrm{rx})} \mid \overline{\mathbb{I}(B, R_I, \mathrm{tx})}\} \cdot \Pr\{\overline{\mathbb{I}(B, R_I, \mathrm{tx})}\}. \quad \text{(B1)}\end{aligned}$$

Based on Property 1, we have that for all $r_I > 0$,

$$\Pr\{\overline{\mathbb{I}(B, R_I, \mathrm{tx})}\} = \exp(-p\lambda\pi R_I^2), \quad \text{(B2)}$$

$$\begin{aligned}\Pr\{\overline{\mathbb{I}(A, r_I, \mathrm{rx})} \mid \overline{\mathbb{I}(B, R_I, \mathrm{tx})}\} &> \Pr\{\overline{\mathbb{I}(A, r_I, \mathrm{rx})}\} \\ &= \exp(-p\lambda\pi r_I^2). \quad \text{(B3)}\end{aligned}$$

In the last inequality, we have used the fact that the logic condition $\overline{\mathbb{I}(B, R_I, \mathrm{tx})}$ reduces the number of primary transmitters that can communicate with primary users within distance r_I of A, which results in a more probable occurrence of $\overline{\mathbb{I}(A, r_I, \mathrm{rx})}$. Then by substituting (B2, B3) into (B1), we have $\Pr[\mathcal{H}_0] > \exp[-p\lambda\pi(r_I^2 + R_I^2)]$ for all r_I.

Obviously, $\Pr[\mathcal{H}_0] \leq \exp(-p\lambda\pi r_I^2)$. Moreover, when $r_I \geq d + R_I + R_p$, we have (see [16])

$$\iint_{\mathcal{S}_c(d,r_I+R_p,R_I)} \frac{\mathcal{S}_I(r, R_p, r_I)}{\pi R_p^2} r\mathrm{d}r\mathrm{d}\theta = \pi(r_I^2 - R_I^2).$$

Thus $\Pr[\mathcal{H}_0] = \exp(-p\lambda\pi r_I^2)$ when $r_I \geq d + R_I + R_p$.

Appendix C: Proof of Proposition 2

From (1, 2), we have

$$\begin{aligned}P_F &= \Pr\{\mathbb{I}(A, r_D, \mathrm{tx}) \mid \mathcal{H}_0\} \\ &= 1 - \Pr\{\overline{\mathbb{I}(A, r_D, \mathrm{tx})} \mid \mathcal{H}_0\}, \quad \text{(C1)} \\ P_{MD} &= \Pr\{\overline{\mathbb{I}(A, r_D, \mathrm{tx})} \mid \mathcal{H}_1\} \\ &= \Pr\{\overline{\mathbb{I}(A, r_D, \mathrm{tx})} \mid \mathbb{I}(A, r_I, \mathrm{rx}) \cup \mathbb{I}(B, R_I, \mathrm{tx})\}. \quad \text{(C2)}\end{aligned}$$

Based on the definition of spectrum opportunity, we have (C3, C4). Since $\Pr[\mathcal{H}_0]$ is known, we only need to calculate the two probabilities in the numerators.

Based on Property 1, we have

$$\Pr\{\overline{\mathbb{I}(A, r_D, \mathrm{tx})}\} = \exp(-p\lambda\pi r_D^2), \quad \text{(C5)}$$

$$\begin{aligned}&\Pr\{\overline{\mathbb{I}(A, r_D, \mathrm{tx})} \cap \overline{\mathbb{I}(B, R_I, \mathrm{tx})}\} \\ &= \exp[-p\lambda(\pi(r_D^2 + R_I^2) - \mathcal{S}_I(d, r_D, R_I))]. \quad \text{(C6)}\end{aligned}$$

By using techniques similar to those used in obtaining $\Pr\{\overline{\mathbb{I}(A, r_I, \mathrm{rx})} \mid \overline{\mathbb{I}(B, R_I, \mathrm{tx})}\}$ (see the proof of Proposition 1 in Sec. III-B), we have (C7). Since $\Pr\{\overline{\mathbb{I}(A, r_D, \mathrm{tx})} \cap \overline{\mathbb{I}(A, r_I, \mathrm{rx})} \cap \overline{\mathbb{I}(B, R_I, \mathrm{tx})}\} = \Pr\{\overline{\mathbb{I}(A, r_I, \mathrm{rx})} \mid \overline{\mathbb{I}(A, r_D, \mathrm{tx})} \cap \overline{\mathbb{I}(B, R_I, \mathrm{tx})}\} \Pr\{\overline{\mathbb{I}(A, r_D, \mathrm{tx})} \cap \overline{\mathbb{I}(B, R_I, \mathrm{tx})}\}$, by substituting (3, C5–C7) into (C3, C4), we obtain (7, 8).

$$\begin{aligned}I(r, R_p, r_I) = &\frac{1}{2}r_I^2 + \frac{r^2}{\pi}\arccos\left(\frac{R_p^2 + r^2 - r_I^2}{2R_p r}\right) + \frac{r_I^2 r^2}{\pi R_p^2}\arccos\left(\frac{r_I^2 + r^2 - R_p^2}{2r_I r}\right) - \frac{r^2}{\pi}\arcsin\left(\frac{r_I^2 + R_p^2 - r^2}{2r_I R_p}\right) \\ &- \frac{r^2 + r_I^2 + R_p^2}{4\pi R_p^2}\sqrt{(r_I + R_p + r)(r_I + R_p - r)(r_I - R_p + r)(R_p - r_I + r)}. \quad \text{(A1)}\end{aligned}$$

$$P_F = 1 - \frac{\Pr\{\overline{\mathbb{I}(A, r_D, \text{tx})} \cap \overline{\mathbb{I}(A, r_I, \text{rx})} \cap \overline{\mathbb{I}(B, R_I, \text{tx})}\}}{\Pr[\mathcal{H}_0]}, \tag{C3}$$

$$P_{MD} = \frac{\Pr\{\overline{\mathbb{I}(A, r_D, \text{tx})}\} - \Pr\{\overline{\mathbb{I}(A, r_D, \text{tx})} \cap \overline{\mathbb{I}(A, r_I, \text{rx})} \cap \overline{\mathbb{I}(B, R_I, \text{tx})}\}}{1 - \Pr[\mathcal{H}_0]}. \tag{C4}$$

$$\Pr\{\overline{\mathbb{I}(A, r_I, \text{rx})} \mid \overline{\mathbb{I}(A, r_D, \text{tx})} \cap \overline{\mathbb{I}(B, R_I, \text{tx})}\} = \exp\left(- \iint_{\mathcal{S}_c(d, r_I + R_p, R_I) - \mathcal{S}_o} p\lambda \frac{\mathcal{S}_I(r, R_p, r_I)}{\pi R_p^2} r \mathrm{d}r \mathrm{d}\theta \right). \tag{C7}$$

$$P_C = \frac{\Pr\{\overline{\mathbb{I}(A, r_D, \text{tx})} \cap \mathbb{I}(A, r_I, \text{rx})\}}{\Pr\{\mathbb{I}(A, r_I, \text{rx})\}} = \frac{\Pr\{\overline{\mathbb{I}(A, r_D, \text{tx})}\} - \Pr\{\overline{\mathbb{I}(A, r_I, \text{rx})} \mid \overline{\mathbb{I}(A, r_D, \text{tx})}\} \cdot \Pr\{\overline{\mathbb{I}(A, r_D, \text{tx})}\}}{\Pr\{\mathbb{I}(A, r_I, \text{rx})\}}. \tag{E1}$$

APPENDIX D: PROOF OF THEOREM 2

Consider first $\frac{r_I}{R_I} \to 0$. As discussed in Sec. II-B, we choose $r_D = R_I$ in this case. Recall that $\mathcal{S}_o = \mathcal{S}_c(d, r_D, R_I) \cap \mathcal{S}_c(d, r_I + R_p, R_I)$ as given in Proposition 2. We then have

$$\lim_{\frac{r_I}{R_I} \to 0} |\mathcal{S}_c(d, r_I + R_p, R_I)| = 0, \qquad \lim_{\frac{r_I}{R_I} \to 0} |\mathcal{S}_o| = 0,$$

$$0 \leq \lim_{\frac{r_I}{R_I} \to 0} \iint_{\mathcal{S}_o} \frac{\mathcal{S}_I(r, R_p, r_I)}{\pi R_p^2} r \mathrm{d}r \mathrm{d}\theta \leq \lim_{\frac{r_I}{R_I} \to 0} \iint_{\mathcal{S}_o} \frac{r_I^2}{R_p^2} r \mathrm{d}r \mathrm{d}\theta = 0.$$

So by substituting the above limits into (7, 8) and applying the continuity of functions in (7, 8), we conclude that $P_F(r_D = R_I) \to 0$, $P_{MD}(r_D = R_I) \to 0$ as $r_I/R_I \to 0$.

Consider next $\frac{r_I}{R_I} \to \infty$. As discussed in Sec. II-B, we choose $r_D = r_I - R_I$ in this case. Then we have

$$\lim_{\frac{r_I}{R_I} \to \infty} \iint_{\mathcal{S}_c(d, r_I + R_p, R_I)} \frac{\mathcal{S}_I(r, R_p, r_I)}{\pi R_p^2} r \mathrm{d}r \mathrm{d}\theta = \pi(r_I^2 - R_I^2),$$

$$\lim_{\frac{r_I}{R_I} \to \infty} \iint_{\mathcal{S}_o} \frac{\mathcal{S}_I(r, R_p, r_I)}{\pi R_p^2} r \mathrm{d}r \mathrm{d}\theta = \pi \left[(r_I - R_I)^2 - R_I^2 \right].$$

Similarly, we can show that $P_F(r_D = r_I - R_I) \to 0$, $P_{MD}(r_D = r_I - R_I) \to 0$ as $r_I/R_I \to \infty$.

APPENDIX E: DERIVATION OF COLLISION PROBABILITY P_C IN PROPOSITION 3

Recall (14) and use the total probability theorem to obtain (E1). It follows from Property 1 that $\Pr\{\mathbb{I}(A, r_I, \text{rx})\} = 1 - \exp(-p\lambda\pi r_I^2)$, $\Pr\{\overline{\mathbb{I}(A, r_D, \text{tx})}\} = \exp(-p\lambda\pi r_D^2)$. Then by using arguments similar to those used in obtaining $\Pr\{\overline{\mathbb{I}(A, r_I, \text{rx})} \mid \overline{\mathbb{I}(B, R_I, \text{tx})}\}$ (see the proof of Proposition 1 in Sec. III-B), we obtain the expression for $\Pr\{\overline{\mathbb{I}(A, r_I, \text{rx})} \mid \overline{\mathbb{I}(A, r_D, \text{tx})}\}$, and (15) follows immediately. Notice that from (15) we can show that P_C decreases as r_D and $p\lambda$ increases [16]. It follows that for fixed r_I, r_D decreases as $p\lambda$ increases in order to satisfy the collision constraint.

REFERENCES

[1] Q. Zhao and B. M. Sadler, "A Survey of Dynamic Spectrum Access," *IEEE Signal Processing Mag.*, vol. 24, no. 3, pp. 79-89, May, 2007.

[2] J. Mitola, III and G. Maguire, Jr., "Cognitive radio: making software radios more personal," *IEEE Personal Commun.*, vol. 6, pp. 13–18, Aug. 1999.

[3] M. Haenggi and D. Puccinelli, "Routing in Ad Hoc Networks: A Case for Long Hops," *IEEE Commun. Mag.*, Oct. 2005.

[4] P. Gupta and P. R. Kumar, "The capacity of wireless networks," *IEEE Trans. Inform. Theory*, vol. 46, March 2000.

[5] M. Krunz, A. Muqattash, and S. J. Lee, "Transmission Power Control in Wireless Ad Hoc Networks: Challenges, Solution, and Open Issues," *IEEE Network*, vol. 48, issue 5, Sep.-Oct., 2004.

[6] J. P. Monks, V. Bharghavan, W. M. Huw, "Transmission Power Control for Multiple Access Wireless Packet Networks," *25th Annual IEEE Conference on Local Computer Networks*, Nov. 2000.

[7] N. A. Pantazis, D. D. Vergados, "A survey on power control issues in wireless sensor networks," *IEEE Commun. Surveys & Tutorials*, vol. 9, issue 4, fourth quarter 2007.

[8] S. Srinivasa and S. A. Jafar, "Soft Sensing and Optimal Power Control for Cognitive Radio," *IEEE 2007 Global Telecommunications Conference*, Nov. 2007.

[9] Y. Chen, G. Yu, Z. Zhang, H. Chen, and P. Qiu, "On Cognitive Radio Networks with Opportunisitic Power Control Strategies in Fading Channels," *IEEE Trans. Wireless Commun.*, vol. 7, no. 7, July 2008.

[10] L. Gao, P. Wu, and S. Cui, "Power and Rate Control with Dynamic Programming for Cognitive Radios," *IEEE 2007 Global Telecommunications Conference*, Nov. 2007.

[11] L. Qian, X. Li, J. Attia, and Z. Gajic, "Power Control for Cognitive Radio Ad Hoc Networks," *15th IEEE Workshop on Local & Metropolitan Area Networks*, June 2007.

[12] M. H. Islam, Y. Liang, and A. T. Hoang, "Joint Power Control and Beamforming for Cognitive Radio Networks," *IEEE Trans. Wireless Commun.*, vol. 7, no. 7, July 2008.

[13] Y. Chen, Q. Zhao, and A. Swami, "Joint design and separation principle for opportunistic spectrum access in the presence of sensing errors," *IEEE Transactions on Information Theory*, vol. 54, no. 5, pp. 2053-2071, May, 2008 (also see Proc. of IEEE Asilomar Conference on Signals, Systems, and Computers, Nov. 2006).

[14] J.F.C. Kingman, "Poisson Processes," Clarendon Press, Oxford, 1993.

[15] A. Martin, "To find the Area Common to Two Intersecting Circles," *the Analyst*, vol. 1, No. 2, pp. 33-34, Feb. 1874.

[16] W. Ren, Q. Zhao, "Opportunity Detection at the Secondary Transmitter and Receiver," Technical Report (TR-07-05), Aug. 2007, http://www.ece.ucdavis.edu/∼qzhao/TR-07-05.pdf.

[17] T. Sheldon, "Encyclopedia of Networking & Telecommunications," Osborne/McGraw-Hill, 2001.

[18] N. Jindal, J. G. Andrews, S. Weber, "Bandwidth Partioning in Decentralized Wireless Networks," *IEEE Trans. Wireless Commun.*, vol. 7, issue 12, part 2, Dec. 2008.

[19] W. Ren, Q. Zhao, D. Cheowtirakul, A. Swami, "Connectivity of Cognitive Radio Networks: Proximity vs. Opportunity," available at http:\\arxiv.org\abs\0903.1684.

Wei Ren (S'07) received the B.Sc. degree in 2003 and the M.Sc. degree in 2006, both from Peking University, China. Now he is a Ph.D. candidate in the Department of Electrical and Computer Engineering, University of California, Davis. His current research interests are in cognitive radio systems and wireless networks. He is also interested in algorithmic theory and optimization techniques for communications.

Qing Zhao (S'97-M'02-SM'08) received the Ph.D. degree in Electrical Engineering in 2001 from Cornell University, Ithaca, NY. In August 2004, she joined the Department of Electrical and Computer Engineering at UC Davis where she is currently an Associate Professor. Prior to that, she was a Communications System Engineer with Aware, Inc., Bedford, MA and a Postdoctoral Research Associate with Cornell University.

Qing Zhao's research interests are in the general area of signal processing, communications, and wireless networking. She received the 2000 Young Author Best Paper Award from IEEE Signal Processing Society and the 2008 Outstanding Junior Faculty Award from the UC Davis College of Engineering. She is an Associate Editor of IEEE TRANSACTIONS ON SIGNAL PROCESSING, and an elected member of IEEE Signal Processing Society SP-COM Technical Committee.

Ananthram Swami (S'79-M'79-SM'96-F'08) received the B.Tech. degree from IIT-Bombay; the M.S. degree from Rice University, and the Ph.D. degree from the University of Southern California (USC), all in Electrical Engineering. He has held positions with Unocal Corporation, USC, CS-3 and Malgudi Systems. He was a Statistical Consultant to the California Lottery, developed a Matlab-based toolbox for non-Gaussian signal processing, and has held visiting faculty positions at INP, Toulouse. He is with the US Army Research Laboratory (ARL) where his work is in the broad areas of signal processing, wireless communications, sensor and mobile ad hoc networks. He is an ARL Fellow.

Dr. Swami is a member of the IEEE Signal Processing Society's (SPS) Technical Committee (TC) on Sensor Array & Multi-channel systems, a member of the IEEE SPS Board of Governors, and serves on the Senior Editorial Board of IEEE Journal of Selected Topics in Signal Processing. He has served as: chair of the IEEE SPS TC on Signal Processing for Communications; member of the SPS Statistical Signal and Array Processing TC; associate editor of the IEEE Transactions on Wireless Communications, IEEE Signal Processing Letters, IEEE Transactions on Circuits & Systems-II, IEEE Signal Processing Magazine, and IEEE Transactions on Signal Processing. He was guest editor of a 2004 Special Issue (SI) of the IEEE Signal Processing Magazine (SPM) on 'Signal Processing for Networking', a 2006 SPM SI on 'Distributed signal processing in sensor networks', a 2006 EURASIP JASP SI on Reliable Communications over Rapidly Time-Varying Channels', a 2007 EURASIP JWCN SI on 'Wireless mobile ad hoc networks', and the Lead Editor for a 2008 IEEE JSTSP SI on "Signal Processing and Networking for Dynamic Spectrum Access". He is a co-editor of the 2007 Wiley book "Wireless Sensor Networks: Signal Processing & Communications Perspectives". He has co-organized and co-chaired three IEEE SPS Workshops (HOS'93, SSAP'96, SPAWC'10) and a 1999 ASA/IMA Workshop on Heavy-Tailed Phenomena. He has co-led tutorials on 'Networking Cognitive Radios for Dynamic Spectrum Access" at ICASSP 2008, DySpan 2008 and MILCOM 2008.